Fluorine atom induced decreases to the contribution of infrared vibrations to the static dielectric constant of Si–O–F alloy films

G. Lucovsky[a] and H. Yang
Departments of Physics, Chemistry, Materials Sciences and Engineering, and Electrical and Computer Engineering, North Carolina State University, Raleigh, North Carolina 27965-8202

(Received 18 February 1997; accepted 31 March 1997)

Si–O–F alloy films deposited by chemical vapor deposition have static dielectric constants, ϵ_s, significantly reduced with respect to those of similarly prepared SiO_2, ~3.2 to 3.4 as compared to 4.0 to 4.2. Infrared absorption spectra provide a basis modeling the molecular structure of these alloys, as well as helping to identify microscopic mechanisms responsible for static dielectric constant reductions. Contributions of electronic and vibrational transitions to ϵ_s are discussed in terms of an empirical chemical bonding model. *Ab initio* calculations are then used to identify inductive effects of Si–F bonds on the properties of Si–O–Si groups that are back-bonded to the Si atom of that Si–F group. The *ab initio* calculations provide a theoretical framework for understanding why relatively low concentrations of F atoms; ~10–12 at. %, produce significant decreases in ϵ_s, ~22%, as reported for the Si–O–F alloys. © *1997 American Vacuum Society.* [S0734-2101(97)12203-5]

I. INTRODUCTION

There is considerable interest in insulating films with static dielectric constants, ϵ_s, lower than SiO_2 for use as dielectric layers between thin film metal interconnects in integrated circuits. One alloy system that has recently attracted considerable attention for this application is Si–O–F. This article

(i) reviews previously published experimental results for the infrared, (IR), optical properties of Si–O–F alloys,[1,2]
(ii) presents new IR data, which when combined with IR data of Refs. 1 and 2, provides the basis for a description of the local bonding arrangements of the incorporated F alloy atoms,
(iii) characterizes the alloy compositions in a pseudo-binary notations,
(iv) explains the major contributing factors to the reductions in ϵ_s atoms by three effects:

(a) replacement of strongly IR-active Si–O–Si with weaker Si–F bonds,
(b) chemical induction effects,[3] whereby Si–F bonds produce changes in frequencies and infrared effective charges of the vibration modes of nearest neighbor Si–O–Si bonding groups reducing the contribution of these modes to the ϵ_s, and
(c) reductions in alloy density.[4]

The reductions in alloy density, ~5% for films with 10–12 at. % F, can only account for about 20% of the total decreases in ϵ_s reported for these films.

On the other hand in Ref. 2 it was demonstrated that decreases in the intensities of Si–O–Si vibrations in the IR absorption spectrum account for a significant fraction of the decreases in the static dielectric constant of Si–O–F alloys with respect to SiO_2. However, no attempts were made in either Refs. 1 or 2 to provide an understanding of *why* these additional decreases in ϵ_s with F alloy atom incorporation were so large. For example, a *one for one* substitution of Si–F bonds for Si–O bonds is insufficient to explain the large changes that occur. In making this comparison, it is necessary to compare integrated absorption strengths rather than simply peak values of the absorption constants of the Si–F and Si–O–Si absorption bands. In this article it is shown that the very large changes in ϵ_s can be understood in terms of additional effects in which the presence of Si–F bonding

(i) reduces the dynamic IR effective charge of nearest-neighbor IR-active Si–O–Si bond-bending vibrations, and
(ii) increases the frequencies of Si–O–Si bond-stretching vibrations.

Both of these contribute to reductions in ϵ_s as will be demonstrated using an extended Penn Model for the quantifying the contributions of the vibrational modes to ϵ_s.[5]

II. INFRARED SPECTRA

The significant changes in IR absorption in Si–O–F alloys with respect to SiO_2 have been documented in Refs. 1 and 2 where IR data has been presented in the spectral range from 400 to 4000 cm^{-1}. This range includes the Si–O and Si–F vibrational modes that make the most significant contributions to ϵ_s; i.e., the Si–O–Si asymmetric bond-stretching mode which peaks at ~1050–90 cm^{-1}, the silicon monofluoride (Si–F) bond-stretching mode at ~935 cm^{-1}, the Si–O–Si bond-bending mode at ~810 cm^{-1}, and the Si–O–Si bond-rocking mode ~460 cm^{-1}. Si–F bond-bending modes are expected at frequencies below 400 cm^{-1}; however, our recent IR measurements shown in Fig. 1 indicate that these are not detectable in alloy films with up to about 12 at. % F. These samples were prepared using conventional direct plasma processing

[a]Electronic mail: gerry_lucovsky@ncsu.edu

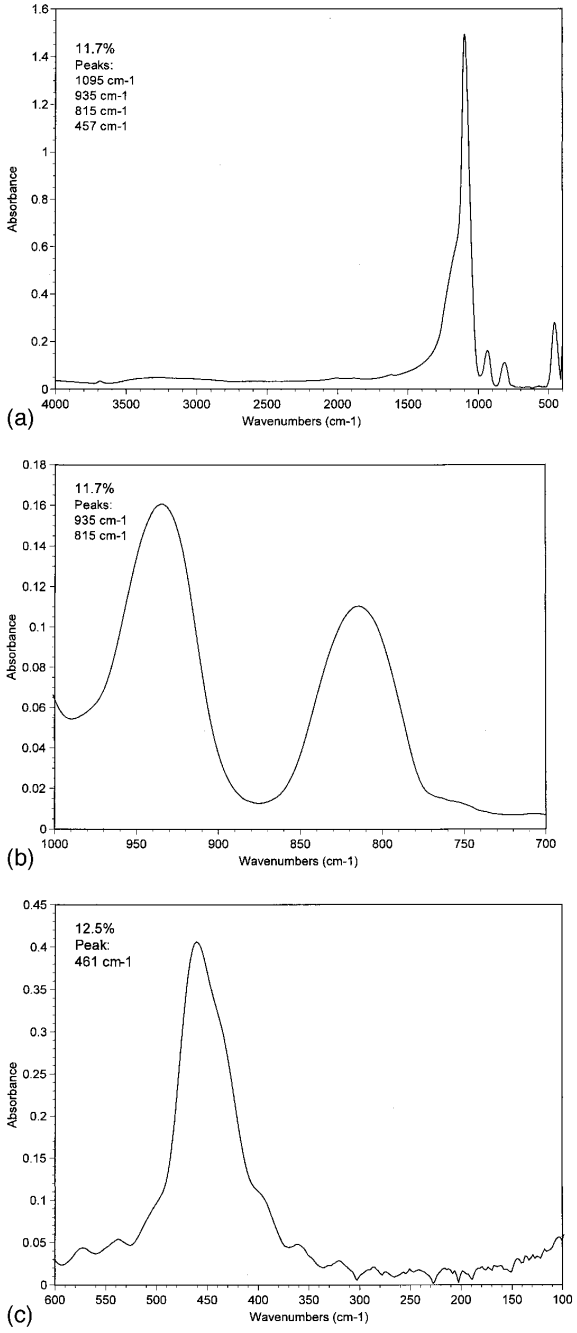

FIG. 1. IR spectra of a Si–O–F alloys: (a) IR spectra from 400 to 4000 cm^{-1} for alloy with 11.7 at. % F; (b) expanded spectrum in the range of the Si–F bond-stretching feature (935 cm^{-1}) and the Si–O–Si bond-bending mode (815 cm^{-1}) for alloy with 11.7 at. % F; and (c) IR spectra from 150 to 400 cm^{-1} for an Si–O–F alloy with 12.5 at. % F. The thicknesses of the alloy films with 11.7 and 12.5 at. % F are essentially the same.

tools, and the F atom concentrations were determined by x-ray photoelectron spectroscopy. The data in Fig. 1 are for samples of approximately the same thickness. We have presented IR data for alloy films, which may then be compared with IR data for SiO_2 films in the corresponding spectral range as presented in Refs. 1 and 2.

Returning first to the data presented in Refs. 1 and 2 include, the most important observations reported for the Si–O–F alloys included the following:

(i) for incorporation of F to about 10–12 at. % there are three significant changes in the IR absorption with respect to SiO_2:
  (a) development of a weak Si–F bond-stretching absorption at $\sim 935\ cm^{-1}$,
  (b) changes in the Si–O bond-stretching band; most notably an increase in the position of the spectral peak with increasing F content, and an accompanying decrease in the half-width, which combine to decrease the integrated IR absorption strength, and
  (c) reductions in the integrated IR absorption strengths of the 810 and 465 cm^{-1} bands with increasing F content;

(i) reductions in ϵ_s from values of $\sim 4.1-4.2$ to 3.3 ± 0.1 for F concentrations of $\sim 10-12$at. %, and

(ii) changes in film properties upon exposure to atmospheric water and low-temperature annealing.

The spectra presented in Fig. 1 show essentially the same changes with respect to SiO_2 spectra as noted above in (i) (a) and (b); e.g., compare the spectra in Fig. 1 with those presented in Ref. 1.

It is important to note that there is no definitive spectroscopic evidence for $Si–F_2$ bonding arrangements in alloys with up to about 12 at. % F in the published literature,[1,2,6] or in the new IR data presented in this article; e.g., in the form of the scissors and rocking bond-bending modes that are anticipated to occur at a frequencies below about 500 cm^{-1}.[7] Returning to bond-stretching modes, Hayasaka *et al.* in Ref. 6 have suggested that the development of low and high wavenumber features on the 935 cm^{-1} Si–F absorption are indicative of the symmetric and anti-symmetric bond-stretching vibrations of $Si–F_2$ bonding groups. The splitting between these two features that they attribute to $Si–F_2$ bonding groups is $\sim 68\ cm^{-1}$ for F concentrations of about 6–8 at. %, and is significantly smaller than what is expected on the basis of kinematic effects for $Si–F_2$ groups from the atomic masses of Si and F.[7] For example, based on the calculations in Ref. 7 a frequency splitting of at least 90 cm^{-1} is expected for the splitting between the symmetric and anti-symmetric $Si–F_2$ vibrations. Finally, in order to confirm unambiguously the presence of $Si–F_2$, it is necessary to show the presence of bond-bending scissors and bond-rocking modes.[7] As noted above, based on the recent IR studies performed in our laboratory which have extended absorption spectra down to 150 cm^{-1}, there is no spectroscopic evidence for either of these types of vibrational modes in samples with up to 12.5 at. % F (see Fig. 1). In addition, the results shown in Fig. 1 also demonstrate that the two additional spectral features reported for the Si–F bond-stretching vibration in Ref. 6 are not *intrinsic* to Si–O–F alloy films. In particular, comparisons with other studies suggest that the 920 cm^{-1} feature reported in Ref. 6 is derived from a reaction of the Si–O–F film with water;[8] i.e., the 920 cm^{-1} fea-

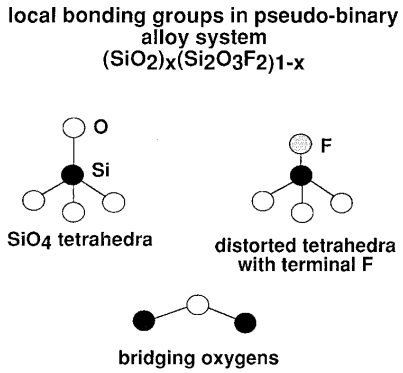

FIG. 2. Local molecular structures in Si–O–F alloys.

ture is due to a displacement of hydrogen bonded OH groups with respect to Si atoms. The results of Ref. 6 showed a distinct feature developed at $\sim 920\ \mathrm{cm}^{-1}$, whereas the presence of a feature at about $980\ \mathrm{cm}^{-1}$ was *inferred* from an attempt to fit the spectral data with three gaussian-shaped bands. Based on the data in Fig. 1, the existence of a discreet mode at $980\ \mathrm{cm}^{-1}$ that is intrinsic to Si–O–F alloys is highly questionable. A similar conclusion can also be drawn from the IR data in Refs. 1 and 2.

Finally, the changes that take place in the position of the spectral peak of the Si–O bond-stretching feature are consistent with the average Si–O–Si bond angle, β, increasing by about 5°–10°, from about 145° in SiO_2 to more than 150° in the Si–O–F alloys. The application of a nearest-neighbor, central force field analysis of the bond-stretching mode indicates that the frequency of this mode is directly proportional to the sine of one-half of the Si–O–Si bond angle; i.e., $\nu = \nu_0 \sin(\beta/2)$, where ν_0 is an empirically determined constant that is approximately equal to the square root of the ratio of a bond-stretching force constant and an oxygen atomic mass.[9]

III. BONDING OF FLUORINE ATOMS IN Si–O–F

The local atomic bonding of univalent atoms and groups in SiO_2 has been previously addressed with emphasis on hydrogen (H) atoms and hydroxyl (OH) groups. In the F-doped SiO_2 alloys, F atoms replace the H atoms or OH groups of hydrogenated SiO_2. As noted above the Si–F bond-stretching vibration is at approximately the same frequency as that the Si–OH vibration, $935\ \mathrm{cm}^{-1}$ as compared to $920\ \mathrm{cm}^{-1}$, consistent with the near equivalence of the masses of F (19 amu) and OH (17 amu). Figure 2 includes a schematic representation of the local atomic bonding of Si–F groups in an SiO_2 host. Based on the arguments presented above, there is no definitive IR spectroscopic evidence for $Si–F_2$ bonding in Si–O–F alloys with concentrations of F up to at least 12 at. %. Therefore, the focus in what follows in based on changes in Si–O–F alloys with respect to SiO_2 that are introduced by the incorporation of monofluoride or Si–F bonding arrangements into the SiO_2 network. The Si–F bond is isoelectronic with the double-bonded P=O group in P_2O_5 glasses, and the Si–F bond-order is also greater than one due to back-donation from filled lone pair-p-orbitals of the F atom into empty anti-bonding states of Si with a d^3s symmetry; i.e., the so-called $p\pi - d\pi$ bonding.[10] The hydroscopic nature of the Si–O–F alloys derives from the high reactivity of the terminal Si–F bond, paralleling the behavior of P=O groups in P_2O_5 glasses and films.

The bonding model presented below has been constructed for an alloy regime in which each Si atom of a host SiO_2 network is bonded to at most one F atom. As noted previously, there is no spectroscopic evidence for multiple attachment of F atoms as in $Si–F_2$ arrangements for the compositions of interest for low-dielectric constant device applications (up to ~ 12 at. % F), so that the bonding model is clearly applicable for these alloy compositions. However to model alloy behavior, it is useful to consider higher F atom concentrations as well. If the monofluoride bonding is taken to the limit of one F atom/Si atom for the *entire* SiO_2 network, then the resulting compound composition is given by $Si_2O_3F_2$ (this composition is an isoelectronic analog of the P_2O_5, which can be written as $P_2O_3(O')_2$ in order to emphasize the two different O bonding environments, three bridging singly bonded oxygen atoms, O, and one terminal doubly bonded oxygen atom designated as O′. Fluorinated oxides with lower concentrations of F can then be described as a homogeneous alloy mixture of SiO_2 and $Si_2O_3F_2$, where a pseudo-binary alloy notation as in $(SiO_2)_x(Si_2O_3F_2)_{1-x}$ is then appropriate. The resulting alloy compositions lie on the join-line between SiO_2 and $Si_2O_3F_2$ in a ternary composition diagram. Note that once the at. % of F is fixed, the ratio of Si to O is also determined. The number of Si–O bonds/Si atom defined by $N_{\mathrm{Si-O}}$ and is equal to $(6-2x)/(2-x)$, and the number of Si–F bonds/Si atom is defined by $N_{\mathrm{Si-F}}$ is equal to $(2-2x)/(2-x)$. Figure 3(a) contains $N_{\mathrm{Si-O}}$ and $N_{\mathrm{Si-F}}$ and Fig. 3(b) contains the atomic fractions, [Si], [O], and [F], all as functions of the alloy composition x. The same model, as shown in Fig. 4, can also be used to calculate the statistical probability for F atoms being

(i) ''isolated'' in the context that they are on Si atoms that are separated by one or more O–Si–O groups,
(ii) at least paired; i.e., on Si atoms that are connected through a single O atom, and
(iii) more strongly clustered in the network structure.

The probability of F atoms being on Si atom sites that are isolated from other F atoms by at least one O–Si–O bonding group is given by $\rho(1-\rho)^3$, where ρ is the fractional occupation of allowed F atom bonding sites. In a similar way the probability of a given F atom having *at least* one nearest-neighbor Si site that is occupied by an F atom is given by $3\rho^2(1-\rho)^2$. It is important to note that the x axes in Figs. 3(a) and 3(b), and Fig. 4 are different. In Fig. 3, they reflect pseudo-binary alloy notation presented above, and in Fig. 4, the x axis is related to the occupancy of available F bonding sites.

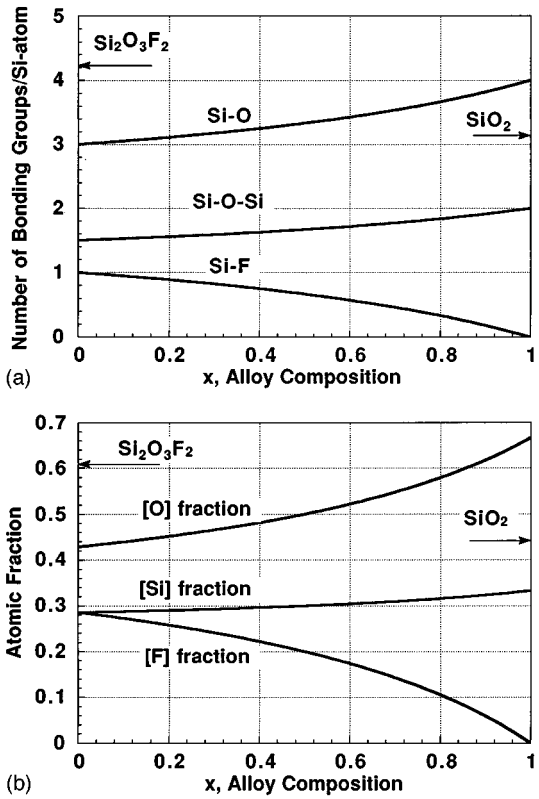

FIG. 3. (a) Concentrations of $N_{\mathrm{Si-O}}$ and $N_{\mathrm{Si-F}}$ bonds and $N_{\mathrm{Si-O-Si}}$ bonding groups, and (b) the atomic fractions, [Si], [O], and [F]; both are plotted as functions of x in the pseudobinary alloy notation.

IV. DIPOLE OSCILLATOR CONTRIBUTIONS TO ϵ_s

In general ϵ_s can be expressed as a sum the contributions of dipole oscillators associated with electronic and vibrational transitions. A representation that is particularly useful is based on a sum of

(i) the optical frequency dielectric, ϵ_0, which includes the integrated contributions from all of the electronic transitions, and
(ii) an additional sum over the contributions from specific types of IR-active vibrations.[2,5]

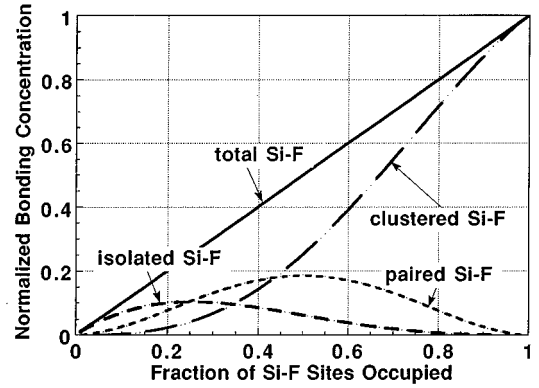

FIG. 4. Isolated and near-neighbor Si–F concentrations as a function of x.

IR studies indicate significant reductions in absorption associated with Si–O–Si bond-stretching modes as F is added to the alloy[1,2] as well as a weak IR response for the Si–F bond-stretching mode, so that the substitution of F for O by itself can lead to a significant reduction in the contribution of the vibrational modes to ϵ_s. ϵ_s can be written as a three-band Penn model[5] as in Eq. (3):

$$\epsilon_s = 1 + \left\{\frac{Ep^E}{Eg^E}\right\}^2 + \left\{\frac{Ep^{V\mathrm{SiO}}}{Eg^{V\mathrm{SiO}}}\right\}^2 + \left\{\frac{Ep^{V\mathrm{SiF}}}{Eg^{V\mathrm{SiF}}}\right\}^2, \tag{3}$$

where

(i) Ep^E is an effective electronic plasma frequency,
(ii) Eg^E is an effective optical band-gap, and
(iii) Ep^{VX} and Eg^{VX} are vibrational frequency analogs of Ep^E and Eg^E, reflecting the separate contributions from $X=$ Si–O and Si–F vibrations.

The vibrational plasma frequencies, Ep^{VX}, represent integrated oscillator strengths that are proportional to the bandwidths and the squares of infrared effective charges, and the vibrational band gaps, Eg^{VX}, are effective vibrational frequencies that are approximately equal to the positions of the respective bond-stretching and bending features in the absorption or ϵ_2 spectra (see Fig. 1 and Refs. 1 and 2). The first two terms in Eq. (3) are defined as the optical frequency dielectric constant, ϵ_0:

$$\epsilon_0 = 1 + \left\{\frac{Ep^E}{Eg^E}\right\}^2. \tag{4}$$

Note that ϵ_0 is the square of the index of refraction, n, which is approximately constant in the transparent region between the band edge and the vibrational absorption bands. Specific relationships between the vibrational and plasma terms in Eq. (4) and vibrational frequencies and IR effective charges can be obtained from

(i) the macroscopic equations that relate transverse optical (TO) and longitudinal optical (LO) frequencies to IR oscillator strengths, and
(ii) the Lydanne, Sachs, Teller relationship as presented for example in Ref. 5.

Note that for disordered materials such as SiO_2 and Si–O–F alloys, the effective TO frequencies are defined by the spectral peaks in the imaginary part of the dielectric function, ϵ_2, and the effective LO frequencies are defined by the spectral peaks in the energy loss function, $\mathrm{Im}(-1/\epsilon)$. The squares of the vibrational plasma frequencies, Ep^{VX}, are proportional to the square of the respective infrared effective charges, and the film density, and the squares of the vibrational band gap terms, Eg^{VX}, are proportional to the squares of the respective transverse vibrational frequencies. These frequencies are integrated averages, and in the spirit of the Penn model, their exact positions are noted necessarily exactly the same as the spectral peaks in the absorption or ϵ_2 spectra.[5] However, for purposes of this article, it is important

to understand that increases in the position of the spectral absorption peaks will also produce increases in the corresponding Eg^{VX} terms.

V. REDUCTIONS IN ϵ_s AS A FUNCTION OF FORMAL BOND IONICITY

To illustrate how ϵ_s scales with an empirically defined bond ionicity, the contributions from electronic and vibrational excitations are presented for a series of Si-based materials in which formal bond ionicity increases: crystalline Si, crystalline Si–C, amorphous SiO_2, and Si_3N_4, and amorphous Si–O–F alloys. An empirically defined ionicity for each of these materials can be characterized by the partial charge on the Si atom that is calculated using the electronegativities of the constituent atoms. This partial charge represents a 'formal' charge transfer from the Si atom in forming chemical bonds to the other compound or alloy constituents; i.e., the larger the electronegativity difference, the larger the partial charge on the Si atom. It is important to note that this partial charge is not equal to an infrared effective charge which, as shown below, generally has both static and dynamic contributions. In addition, and more importantly, following the original definition of electronegativity as put forth by Pauling, the larger the partial charge on the Si atom, the more ionic the bonding in the context of heteropolar contributions to the total bond energy.[10]

Using the Sanderson method of Ref. 11, an effective electronegativity (X'_A) can be calculated for each of the materials in a compound (A_nB_m) according to the relationship presented below in Eq. (5):

$$X'_A = X'_B = [(X_A)^n (X_B)^m]^{1/(n+m)}, \tag{5}$$

where A is taken to be Si, and B is the other atomic constituent; e.g., C, N, O or F. Using the values of X'_{Si} for Si from Eq. (5), the Si-atom partial charge, e_{Si}, is then calculated from:

$$e_{\mathrm{Si}} = \frac{X'_{\mathrm{Si}} - X_{\mathrm{Si}}}{2.08(X_{\mathrm{Si}})^{0.5}}, \tag{6}$$

where X_{Si} is the electronegativity of a Si atom in a purely covalent bond, as in crystalline Si.[11] Equation (6) is an empirical relationship that is based on defining effective charges for Na and F in NaF that are consistent with the fractional ionicity of that material (see details in Ref. 8). The values of e_{Si} for materials other than crystalline Si considered in Figs. 5(a) and 5(b) are positive indicating electrons are withdrawn from the Si atom when it bonds to species such as C, N, O and F which have values of electronegativity that are greater than that of Si; i.e., from Eq. (5) X'_{Si} is larger than X_{si}, so that e_{Si} is positive. Figure 5(a) contains plots of experimentally determined values of ϵ_0 and ϵ_s as functions of the Si atom partial charge; $\epsilon_0 = n^2$, where n is the index of refraction. The difference between ϵ_s and ϵ_0 is due primarily to the contributions from the vibrational modes and is shown in Fig. 5(b). In some molecular systems there are also contributions to ϵ_s from very low frequency dipolar effects; however, there is no evidence that these contributions are significant in inorganic materials such as SiO_2 and Si_3N_4. Returning to the IR active vibrational modes, as the partial charge of the Si atom increases, the contribution of the vibrational modes to ϵ_s in Fig. 5(b) decreases. This observation is counter-intuitive in as much as it sometimes assumed that the strength of IR active modes increases as the bond ionicity increases. Many studies have shown that this is not the case; e.g., the IR active modes in homopolar trigonal Se and Te crystals make contributions to the static dielectric constant well in excess of those of ionic crystal such as NaCl.[12] This derives from the fact that the IR effective charges, that characterize the IR strengths have both static contributions, that can sometimes correlate with bond ionicity as defined above, as well as dynamic contributions that come from charge redistribution during the course of the vibrational motion (see discussion below). For Se and Te the effective charges are entirely dynamic and are significantly larger than the effective charges in ionic materials such as NaCl and other rocksalt structured crystals.[12]

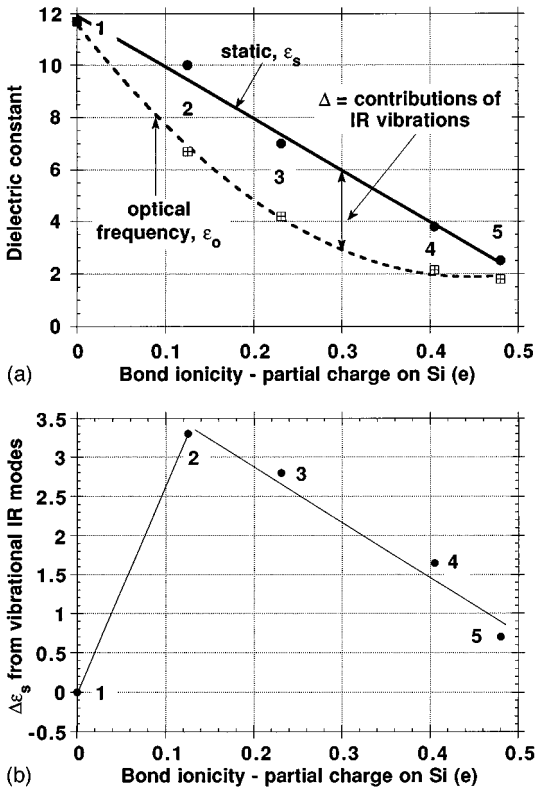

FIG. 5. Plots of (a) ϵ_0 and ϵ_s and (b) the contribution to ϵ_s from the vibrational modes, both as functions of the Si atom partial charge for: **1** crystalline-Si, **2** β-SiC, **3** noncrystalline Si_3N_4, **4** noncrystalline SiO_2, and **5** extrapolated approximate values for $Si_2O_3F_2$. The values of $\epsilon_0 (= n^2)$ and ϵ_s are experimental.

As noted above the contribution of a vibrational mode to ϵ_s depends on the ratio of a plasma frequency to a vibrational band gap or average TO frequency. Two factors contribute to the trend in Fig. 5(b)

(i) decreases in the IR effective charge with increasing bond ionicity, and

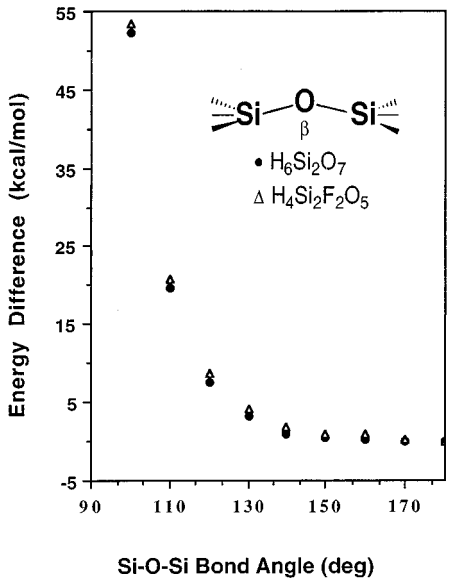

FIG. 6. Excess energy with respect to optimum energy as a function of Si–O–Si bond angle, β. This diagram contains a schematic representation of the two molecular structures used in the *ab initio* calculations.

(ii) increases in the effective TO frequency with increasing ionicity.

The decreases in the IR effective charges reduce the vibrational effective plasma frequencies and the increases in the effective TO frequencies increase the effective vibrational band gaps. Referring to Eq. (3), these changes both contribute to decreases in ϵ_s. As shown in Sec. VI, there are two factors related to effective charges contribute to the decreased IR contributions

(i) the IR effective charge of a Si–F vibration is smaller than that of the Si–O–Si vibration that it replaces, and
(ii) the incorporation of a Si–F bond to a Si atom that is back-bonded to three O atoms can reduce the IR effective charges of the back-bonded Si–O–Si groups.

A third factor derives from a significant increase in the frequency of the bond-stretching Si–O–Si upon alloying with F. It is important to recognize that in applying the extended Penn model of Eq. (3), that the plasma frequency terms represent integrals over vibrational bands, e.g., the bending, stretching, and rocking modes of SiO_2, and as such are not simply proportional to the peak values of the respective absorption constants.

VI. RESULTS OF *AB INITIO* CALCULATIONS

The details of the *ab initio* calculations for the effects identified immediately above in (i) and (ii) will be presented elsewhere.[13] At this time, we will simply indicate the important results for

(i) the energy difference between the minimum value for a 180° Si–O–Si bond angle (β) and other bond angles down to the 100° in Fig. 6, and
(ii) the changes in the IR effective charges for the Si–O–Si bond-stretching, bending, and rocking vibrations in Fig. 7 that are induced by F atom induction effects in Fig. 7.

Figure 6 displays the energy difference between the minimum value for a 180° Si–O–Si bond angle (β) and other bond angles down to 100°. A schematic representation of the local clusters used in this calculation is included. There is no significant difference in this energy difference for Si–O–Si bond angles between about 130° and 180°, consistent with x-ray diffraction studies of glassy SiO_2 which indicate an average bond angle of about 150°, and a bond angle spread of about 50°.[14] Most importantly for purposes of this study this difference is in the variation of this energy difference function for H terminated and F terminated clusters.

The IR effective charges presented in Figs. 7(a), 7(b) and 7(c) are computed numerically by calculating changes in the dipole moments (M) corresponding to displacements (u) of the O atom and F atoms that are appropriate to their respective bonding stretching vibrations; i.e., the O atom is displaced in direction parallel a line joining its two Si atom neighbors, and the F atom is displaced along the Si–F bond. The IR effective charge (e^*) is associated with a redistribution of the electrons that results from these displacements, and is given by the following expression:

$$e^* = \delta M / \delta u, \tag{7}$$

where the derivative is evaluated in the limit of small displacements of u; i.e., one calculates the moment, M, as a function of the displacement coordinate, u, and then determines the derivative in the limit of small displacements. This calculation is not in any way based on the definition of partial charge as determined from the atomic electronegativities, nor is it expected that the IR effective charge should be equal to the IR effective charge. The IR effective charge is a derivative property of the local atomic structure, whereas the partial charge is a static property that is directly related to ionic contributions to the total bond energy. The contribution of a vibrational mode to ϵ_s is proportional to the square of this effective charge and these are the quantities presented in Fig. 7. Note that the bond angles of interest are from about 120°–180° degrees.

Consider first the bond-stretching modes: the square of the IR effective charge for this mode

(i) is a strong function of the Si–O–Si bond angle, increasing by more than a factor of 2 as the bond angle is increased from about 120° to 180° and
(ii) is reduced by about the same amount for all angles by F addition.

The effective charge of the bond-bending mode shows a complementary behavior, decreasing by about 30% as the bond angle is increased. As in the case of the bond-stretching mode, the addition of F reduces the effective charge for all Si–O–Si bond angles considered; however the decrease be-

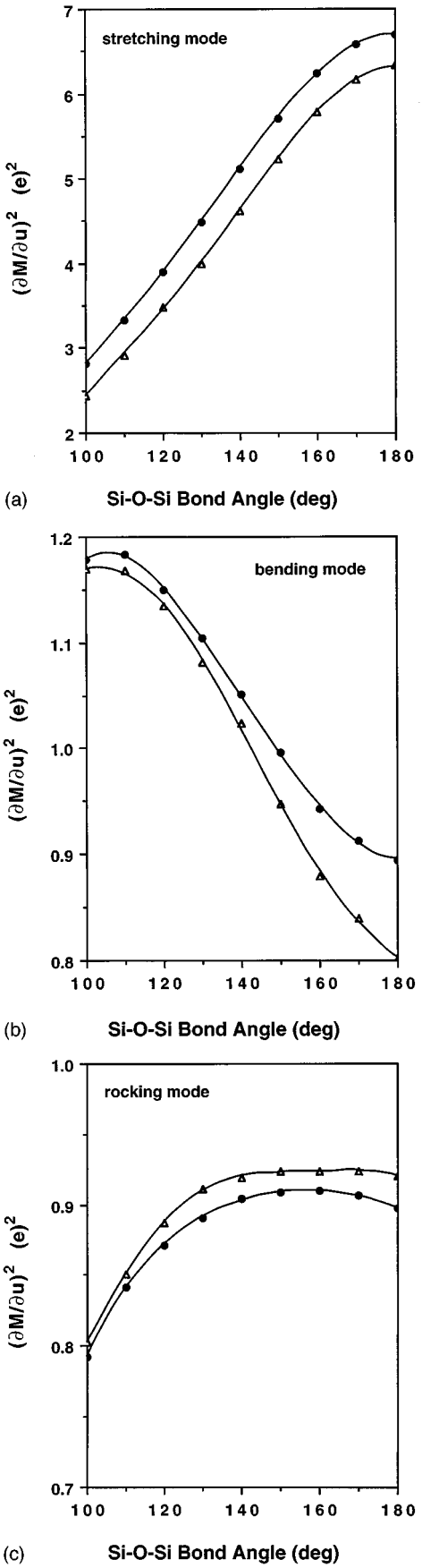

FIG. 7. Squares of the IR effective charges for (a) bond-stretching, (b) bond-bending, and (c) bond-rocking modes as a function of the Si–O–Si bond angle. The diagrams contain comparisons.

comes much greater as the Si–O–Si angle increases. Finally, the effective charge for the bond-rocking mode shows a qualitatively different behavior

(i) there is a small increase in the effective charge for the fluorinated case, and
(ii) the variation of the effective charge with Si–O–Si bond angle is significantly smaller than the for the bond-bending and bond-stretching modes, particularly for bond angles between about 120° and 180°.

With regard to the relative magnitudes of the effective charges, the bond-bending and bond rocking modes are have similar effective charges, $\sim 1\,e$ in magnitude, whereas the effective charge for the bond-stretching mode is significantly greater, $\sim 2-2.5\,e$ for Si–O–Si bond angles in the vicinity of 150°. The relative magnitudes of the squares of the calculated effective charges for the three vibrational modes of SiO_2 are in excellent agreement with the integrated strengths of the respective IR bands.

From the experimental data presented in Refs. 1 and 2 and the results in Fig. 1, it is obvious that the reduction in the Si–O–Si vibrational mode contributions to ϵ_s from the substitution of one F atom for one O atom is insufficient to account for the relatively large decreases in ϵ_s. For example, in a 12 at. % F alloy which exceeds the concentration discussed above, about 10% of the Si–O–Si groups are removed, and the maximum decrease in ϵ_s from removal of these groups is about 10% of $\delta\epsilon = 0.1(\epsilon_s - \epsilon_0) \approx 0.10(4.1-2.1)$ or ~ 0.2, whereas the reported decrease in ϵ_s is approximately 0.8. This zeroth order calculation actually overestimates the effect for the bond-stretching modes, where the modes most effected are those with the smallest bond angles and the smallest IR moments. The reverse is true for the bond-bending modes, and the anticipated fractional decrease in this mode at $\sim 800\ \mathrm{cm}^{-1}$ is readily evident in the IR spectra (see Refs. 1 and 2). Since the square of the moment of bond-stretching modes of the Si–O–Si groups bonded to a Si–F are reduced by the addition of that F neighbor, this adds significantly to the decrease in e_s. Since for 40% occupancy of the available Si atom bonding sites, each Si–O–Si groups is in bonding contact with at least one F atom, this mechanism contributes to an additional decrease of about 0.05, that is in part offset by the shift in the centroid of the bond-stretching modes to higher wave number. Combined with the decreased contributions from the Si–O–Si bending modes which contribute to an additional decrease in ϵ_s of ~ 0.1, this approach goes far in accounting for the behavior of ϵ_s with increasing F content. However, to be more quantitative, two additional factors must be taken into account. One additional factor is the increase in the vibrational frequency of the Si–O–Si bond-stretching mode [see Eq. (2)]. For example, increasing the average frequency of the Si–O–Si bond-stretching vibration from 1060 to $1090\ \mathrm{cm}^{-1}$ will decrease the fractional contribution of these modes to ϵ_s by $\sim 6\%$, or about 0.15. Since these modes make the largest contribution to ϵ_s, this change is indeed significant. Finally, as noted above, the reduction in alloy

density, ~5% for an alloy with 10–12 at. % F also contributes a factor of ~0.2.[4] Combining these terms then explains a total decrease in ϵ_s of about 0.7, as compared to the experimental value of 0.8. Combining these terms then explains the significant decreases in ϵ_s. The quantitative agreement validates the accuracy of the theory and the use of relatively small molecular clusters to obtain properties of vibrational modes in continuous random networks.

The calculation presented above identifies the answer to the apparent paradox between increases in the Si partial charge and decreases in the contribution of vibrational modes to ϵ_s. We had shown in Figs. 5(a) and 5(b) that the contribution of vibrational modes to ϵ_s decreased with increasing *partial charge* on the Si atom. It must be noted that this partial charge is merely an empirical way of characterizing chemical bonding effects associated with electronegativity changes induced by near-neighbor atoms. The validity of this approach is borne out by the scaling of vibrational frequencies of Si–H (Ref. 5) and P=O (Ref. 10) vibrations, and deep level core shifts as monitored by x-ray photoelectron spectroscopy.[10] On the other hand, this partial charge is not necessarily equal to, or even proportional to the IR effective charge. The large IR effective charges, ~2.5*e* for bond angles of about 150°, are significantly larger than e_{Si}. From the *ab initio* calculations, it is evident that the large IR charge for the asymmetric bond-stretching vibration is due to a dynamic effect rather than static charge transfer. On the other hand, the smaller IR effective charge for the bond-rocking mode is due mostly to static charge transfer. The *ab initio* calculations also provide direct evidence for the back donation of electrons from the F atom to the Si atom, confirming the empirical chemistry arguments for a $p\pi-d\pi$ component of the Si–F bonding. This is the effect which serves to reduce the dynamic effective charge of the Si–O–Si groups when F nearest neighbors are present.

VII. REACTION PATHWAYS TO FLUORINE ATOM INCORPORATION

There are two possible reaction pathways to F atom incorporation in the SiO_2 materials:

(i) development of an SiO_2 network structure with subsequent attack by F, or
(ii) the development of the Si–O–F network directly.

The major effects of the added F atoms on the SiO_2 network as exemplified by the IR is the shift of the Si–O–Si bond-stretching frequency to higher wave numbers and the accompanying reduction of the spectral width of that feature. Since the spectral peak absorbance of the bond-stretching mode in the fluorinated films is higher than the absorbance at the same wave number in the film without any F (see Fig. 1 and IR data in Ref. 1), this means that the second mechanism applies; that is the IR absorption in the fluorinated film is not simply related to removing some of the oscillators that contribute to that band. The situation is different in SiO_2 films that have been attacked by water vapor.[8] In particular, the first mechanism applies to the attack by water of low temperature, low density SiO_2 films prepared by plasma deposition.[6] This post deposition process is characterized by its reversible character as well.

VIII. DISCUSSION

The main points of this article are

(i) for relatively small additions of F to SiO_2, up to 12 at. %, there are relatively large changes in ϵ_s,
(ii) alloy compositions with small additions of F can be described in terms of a pseudobinary notation, $(SiO_2)_x(Si_2O_3F_2)_{1-x}$, from which alloy atom and bonding configurations can be computed;
(iii) the primary factor contributing to decreases in ϵ_s in these alloys is a decrease in the contributions from the vibrational modes;
(iv) the replacement of O with F has two effects on the IR effective charges which determine the absorption strengths:
  (a) Si–F vibrations have lower e^*'s for the dominant bond-stretching modes than Si–O vibrations, and
  (b) the increased partial charge on the Si reduces the e^*'s of the both the bond-stretching and bond-bending vibrations Si–O vibrations;
(i) the hydroscopic nature of the Si–O–F alloys is related to Si–F bonding, predominantly near-neighbor Si–F groups; and
(ii) there are no other inorganic dielectrics based on alloy formation with SiO_2 that can yield lower values of ϵ_s, so that the alloy approach to the so-called low-*k* dielectrics is limited to reductions of ϵ_s to values between 3.2 and 3.4.

ACKNOWLEDGMENTS

This work is supported by ONR, National Science Foundation, SRC, and Intel Corporation.

[1]S. W. Lim, Y. Shimogaki, Y. Nakano, K, Tada, and H. Komiyama, *Extended Abstracts of the 1995 International Conference on Solid State Device and Materials* (Business Center for Academic Societies Japan, Tokyo, 1995), p. 153.
[2]S. W. Lim, Y. Shimogaki, Y. Nakano, K. Tada, and H. Komiyama, Jpn. J. Appl. Phys. **135**, 1468 (1996).
[3]G. Lucovsky, AIP. Conf. Proc. **75**, 100 (1981), and references therein.
[4]D. T. Hodul, MRS Symp. Proc. (in press).
[5]G. Burns, *Solid State Physics* (Academic, New York, 1985).
[6]N. Hayasaka, H. Miyajima, Y. Nakasaki, and R. Katsumaa, *Extended Abstracts of the 1995 International Conference on Solid State Device and Materials* (Business Center for Academic Societies Japan, Tokyo, 1995), p. 157.
[7]G. Lucovsky, in *Fundamentals Physics of Amorphous Semiconductors*, edited by F. Yonezawa (Springer, Berlin, 1980), p. 87.
[8]J. A. Theil, D. V. Tsu, S. S. Kim, and G. Lucovsky, J. Vac. Sci. Technol. A **8**, 1374 (1990).
[9]G. Hertzberg, *Infra-red and Raman Spectra of Polyatomic Molecules* (Van Nostrand, New York, 1945).
[10]J. E. Huheey, *Inorganic Chemistry* (Harper and Row, New York, 1978).
[11]R. T. Sanderson, *Chemical Bonds and Bond Energy* (Academic, New York, 1971).
[12]E. Burstein, M. H. Brodsky, and G. Lucovsky, Int. J. Quantum Chem. **1s**, 759 (1967).
[13]H. Yang, G. Lucovsky, and J. L. Whitten (unpublished).
[14]R. L. Mozzi and B. E. Warren, J. Appl. Crystallogr. **2**, 164 (1969).